Journal of Macromolecular Science, Part A
Publication details, including instructions for authors and subscription information:
http://www.informaworld.com/smpp/title~content=t713597274

Exploration of Novel Pyrene Labeled Amphiphilic Block Copolymers: Synthesis Via ATRP, Characterization and Properties

Neelamegan Haridharan[a]; Venkatachalam Ramkumar[a]; Raghavachari Dhamodharan[a]
[a] Department of Chemistry, Indian Institute of Technology Madras, Chennai, India

Online publication date: 30 July 2010

To cite this Article Haridharan, Neelamegan , Ramkumar, Venkatachalam and Dhamodharan, Raghavachari(2010) 'Exploration of Novel Pyrene Labeled Amphiphilic Block Copolymers: Synthesis Via ATRP, Characterization and Properties', Journal of Macromolecular Science, Part A, 47: 9, 918 — 926
To link to this Article: DOI: 10.1080/10601325.2010.501681
URL: http://dx.doi.org/10.1080/10601325.2010.501681

Journal of Macromolecular Science, Part A: Pure and Applied Chemistry (2010) **47**, 918–926

ISSN: 1060-1325 print / 1520-5738 online
DOI: 10.1080/10601325.2010.501681

Exploration of Novel Pyrene Labeled Amphiphilic Block Copolymers: Synthesis Via ATRP, Characterization and Properties

NEELAMEGAN HARIDHARAN, VENKATACHALAM RAMKUMAR and RAGHAVACHARI DHAMODHARAN*

Department of Chemistry, Indian Institute of Technology Madras, Chennai, India

Received January 2010, Accepted April 2010

A novel initiator containing pyrene, a fluorescent moiety, was prepared by reacting 1-aminopyrene and 2-bromoisobutyl bromide. The structure elucidation of the new initiator was carried out using various spectroscopic tools, as well as through single crystal X-ray diffraction studies. Novel, fluorescent amphiphilic block copolymers with a pyrene end-group, poly(styrene-*b*-acrylic acid) [P(S-*b*-AA)], poly(methyl methacrylate-*b*-dimethylaminoethyl methacrylate) [P(MMA-*b*-DMAEMA)], poly(styrene-*b*-*tert*-butyl acrylate) [P(S-*b*-*t*-BA)], poly(styrene-*b*-dimethylaminoethyl methacrylate) [P(S-*b*-DMAEMA)] were successfully synthesized by the atom transfer radical polymerization (ATRP) method, using CuBr as the catalyst and N,N,N′,N″,N″-pentamethyldiethylenetriamine (PMDETA)/N,N,N′,N″,N″-hexamethyltriethylenetetramine (HMTETA) as the complexing agent. The polymers were characterized by GPC, ^{1}H-NMR, IR and UV-Vis spectroscopies. It was observed that as the polymerization time increased, both the conversion and the molecular weight increased linearly with time. The fluorescence properties of the polymers prepared were recorded. The physical properties and especially the pH dependent swelling properties of the amphiphilic block copolymers have been investigated. The utility of the block copolymers in the formation of stable dispersion of cadmium sulphide nanoparticles was investigated as a model study.

Keywords: Amphiphilic block copolymer, atom transfer radical polymerization (ATRP), fluorescent polymers, fluorescent ATRP initiator, fluorescence, pyrene, swelling

1 Introduction

One of the most important goals in synthetic polymer chemistry is to gain control over not only the molecular weight and polydispersities of polymer chain, but also their composition, architecture and end group functionalities (1). The living free radical polymerization offers a powerful tool to synthesize polymers with pre-designed structures. The most widely used living radical polymerization are stable free radical polymerization (SFRP) (2), atom transfer radical polymerization (ATRP) (3–5) and reversible addition fragmentation chain transfer (RAFT) polymerization (6). The ATRP polymerization has been considered as one of the most versatile controlled/living radical polymerizations, since it has proven to be effective for a wide range of monomers (styrene, (metha)acrylates, acrylonitrile, etc.). ATRP reactions have been performed under ambient conditions (us) (7, 8) and thus, it is a versatile tool to produce novel materials.

Recently, much attention has been devoted to the polymers with fluorescent moiety due to their potential in biological and optical applications (9). To prepare such polymers with fluorescent moiety, different fluorophores can be attached to the monomers or to an initiating group. Pyrene containing polymers are of great interest because of their potential use as semiconductors, photoresist materials and fluorescent probes (10). Various methods have been developed to attach pyrene moieties to polymers. Pyrene compounds and pyrene containing polymers are attracting interest because of their excellent fluorescence and long lived excited state and are used as a fluorescent probe, in labeling (chromophore), for detecting fluorescence, in optoelectronic devices and in drug delivery vesicles (11,12).

Zhang et al., reported on the use of pyrene loaded biodegradable polymer nanoparticles by incorporating pyrene into the polymer nanoparticles formulated from amphiphilic diblock copolymer. These were utilized as a fluorescent marker for medicinal purposes (13). Winnik

*Address correspondence to: Raghavachari Dhamodharan, Department of Chemistry, Indian Institute of Technology Madras, Chennai 600 036, India. Tel: 91-44-2257 4204; Fax: 91-44-2257 4202; E-mail: damo@iitm.ac.in

et al., reported on the interactions of poly(N-isopropyl acrylamide) with liposomes using pyrene labeling (14). Nakayama and Okano (15), as well as Scales et al., (16) reported on the synthesis and properties of pyrene end-capped polymers via RAFT polymerizations. Laukkanen et al., reported on the aggregation behavior in water of a thermosensitive graft copolymer of vinyl caprolactam and poly(ethylene oxide) with alkyl methacrylate macromonomer using pyrene labeling (17). Yagci et al., reported on the diffusion processes of pyrene end-capped polystyrene in gels (18). Recently, Liaw et al., reported on the self- assembly of fluorescent amphiphilic CBABC type pentablock copolymers containing pyrene pendant group in one of the monomers (19).

Atom transfer radical polymerization (ATRP) is one of the more efficient controlled/living radical polymerization (CLRP) methods since its introduction in 1995 (20). One of the advantages of ATRP is that the molecular weight and functionality can be controlled. It can also tolerate a wide range of functional groups, in the initiator (21), monomer and the solvent. One of the major challenges to conquer in the field of metal catalyzed living radical polymerization is the enhancement of the rate of polymerization with preservation of the control of the molecular weight and polydispersity (M_w/M_n) (22). For controlled polymerization under mild conditions such as at room temperature, it is important to choose a suitable organic halide initiator and a catalyst system.

Amphiphilic block copolymers have great application potential eg: in the dispersions, separations and also as drug and gene delivery vehicles (23). They also have wide application potential in micro reactor chemistry, pharmacology, medicine and cosmetics. Amphiphilic block copolymers form micelles and bilayer residue in solution and micro phase- separated solids and as such they find applications as surfactants, flocculants and nanosized reactors. The interest in the synthesis and characterization of amphiphilic block copolymers has increased enormously in recent years. This is mainly attributed to the difference in chemical nature within a macromolecule, constituting amphiphilicity as one of the characters. The physical property of amphiphilic block copolymers has been investigated by a number of researchers. Amphiphilic block copolymers have the property to swell in water and aqueous solution during which state, they are soft and rubbery, resembling living tissues.

In recent years, amphiphilic block copolymers have also been used as a stabilizing agent for nanoparticles synthesis. Due to their amphiphilic nature, they have found important biological applications as controlled gene and drug encapsulation and delivery systems (24). CdS nanoparticles is one of the most intensively investigated semiconducting nanoparticles. CdS nanoparticles have been synthesized on many kinds of templates such as polymers, zeolites, etc. Recently, researchers developed cadmium sulphide nanoparticles through amphiphilic block copolymers due to their unique size dependent chemical and physical properties (25). Chen et al. reported on the formation of micelles with corona-embedded CdS nanoparticles based on complex formation between DMAEMA units and cadmium ions, using amphiphilic triblock copolymer (26). In this article, we report the stabilization of CdS nanoparticle using novel fluorescent pyrene based amphiphilic block copolymers and study its swelling behavior at various pHs.

2 Experimental

2.1 Materials

All the monomers used here (styrene, methyl methacrylate, dimethylaminoethyl methacrylate, *tert*-butyl acrylate) were purchased from Aldrich and were passed through an Al_2O_3 column before use. Bromoisobutryl bromide, copper(I) bromide, copper(I) chloride, 1-amino pyrene, trifluoroacetic acid, anisole and PMDETA/HMTETA were purchased from Aldrich and were used as received. Cadmium acetate dihydrate and sodium sulphide was purchased from Lancaster chemicals. Triethyl amine, tetrahydrofuran (THF) and dimethyl formamide (DMF) were distilled, before use.

2.2 Methods

The ^{1}H-NMR and ^{13}C-NMR spectra were recorded on a Bruker Avance 400 spectrometer, (100 MHz for ^{13}C) and were measured in $CDCl_3$ or D_2O (wherever applicable), at room temperature. The high resolution Scanning Electron Microscopy (SEM) was performed using a FEI Quanta 200 Scanning Electron Microscope.

The FT-IR spectra were recorded on a Nicolet FT-IR 6700 spectrometer. UV-Visible absorbtion spectra were measured on a JASCO UV-Visible 530 spectrometer. The mass spectrum was performed using a Q-TOF micromass spectrometer (WATERS) with electrospray ionization. The TGA were recorded on a ThermoGravimetric Analyser TGA 7 in the temperature range 50–800°C at a heating rate of 20°C/min under flowing nitrogen (high purity) gas. The molecular weight data were recorded on a WATERS GPC equipped with three columns of average pore size 10^3, 10^4, 10^5 Å and connected in series. Tetrahydrofuran (THF) was used as the eluent, at the flow rate of 1 ml/min. Detection was performed using a refractive index detector (2410 WATERS). Narrow molecular weight polystyrene (PS) standards were used for calibration and data analysis was performed using Empower software (WATERS). Fluorescence spectra were recorded on a HITACHI F-4500 spectrofluorimeter under the following conditions: excitation wavelength 337 nm, emission wavelength of 390 nm, scan speed - 2400 nm/min, excitation and emission slit width of 5.0 nm. Single crystal X-ray diffraction analysis was performed on a Bruker X8 Kappa APEX II

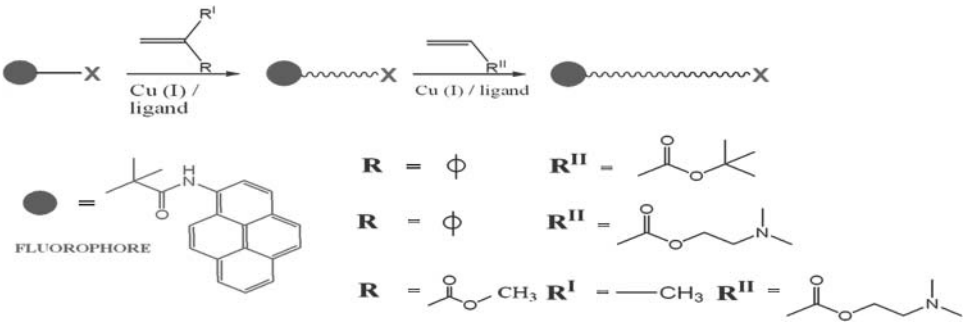

Sch. 1. Pictorial representation of the synthesis of block copolymer fluorophores.

Diffractometer. Powder X-ray diffraction analysis was performed on a Bruker Discover D8 Diffractometer (Cu anode and 2θ horizontal goniometer).

2.3 X-Ray Crystallographic Measurements

The X-Ray crystallographic measurements of the pyrene based initiator was carried out on a Bruker (Kappa APEX II) diffractometer equipped with graphite monochromator Mo-Kα radiation. The data were collected with 99.8% completeness for theta up to 25 deg for Mo-Kα radiation. ω and φ scans was employed to collect the data.

For single crystal X-ray diffraction studies, the crystals of the pyrene based ATRP initiator, suitable for X-ray analysis, were grown by the method of slow evaporation from hexane to achieve good quality single crystals. Additional material is available from the Cambridge Crystallographic Data Center from deposit@ccdc.com.ac.uk, ref code CCDC 730925. The molecular formula of the initiator is C_{20} H_{16} Br N O and the molecular weight is 366.25 g mol^{-1} (mass spectrometry). The structure is found to be monoclinic, with space group P21/c, a = 26.226 (3), b = 6.1707(8), c = 9.9831(12), $\beta = 96.228(4)$. V = 1606.1(3)A^3, Z = 4, $\rho_{calc} = 1.515$ g/cm^3. The X-ray powder diffraction (XRD) pattern was recorded on a Bruker Discover D8 Diffractometer with Cu anode and 2Theta horizontal goniometer, employing scanning rate of 0.1deg/s in 2θ range from 20 to 70°. The polymer for powder x-ray analysis were mounted on a glass slide (petroleum jelly supported) and scanned in the region of 5 to 70 degrees (2θ values).

2.4 Synthesis of Pyrene-based Initiator

1-aminopyrene (0.04 mols), triethylamine (0.044 mols) and THF (400 ml) were placed in a three- neck round bottomed flask. Bromoisobutyrl bromide (0.044 mols) was added slowly, using a syringe, with stirring, upon which an orange precipitate of triethylammonium bromide was formed. The mixture was left to react for 6 h, with stirring. Subsequently, triethylammonium bromide, the precipitate was removed by filtration and the THF was removed by rotary evaporation. The product was purified by column chromatography technique resulted as a white solid which was characterized by NMR, IR, and MASS spectroscopic methods.

Yield: (14.64g: 85%); melting point = 190–192°C; ^{1}H-NMR (400 MHz, $CDCl_3$, δ, ppm): 2.2 (s, 6H, -C $(CH_3)_2$-), 9.2 (s, 1H, -NH-), 7.9–8.5 (m, 9H, aromatic protons); ^{13}C-NMR (100 MHz, $CDCl_3$, δ, ppm): 31.2 (aliphatic CH_3 carbon), 54.7 (aliphatic carbon attached to carbonyl group), 82.3, 119, 126, 151, 155 (quaternary carbon), 110, 118.1, 119, 125.7, 126.3, 127.6, 129.3, 131.5, 135.7, 151.6, 155.8 (aromatic –CH- carbons), 169, 170 (carbonyl carbon, -O-C=O); DEPT (400 MHz, $CDCl_3$, δ, ppm): The presence of CH_3 protons around 30 ppm and –CH- protons around 120–130 ppm is clearly identified; FT-IR (NEAT cm^{-1}): 3400–3500 (broad -N-H), 2928 ((s) overtones aliphatic groups), 2050, 1079 ((s) C-O-C), 892.3,1611 ((m) C-C aliphatic), 1758.6 ((s) C=O, ester from the initiator); TOF-MS (m/z) : The peaks appearing at m/z 368 and 366 (M^+ $C_{20}H_{16}OBrN$; molecular ions) confirmed the structure of the initiator.

2.5 Typical ATRP Procedure

The required quantity of the copper catalyst was added to a flame dried Schlenk tube equipped with a magnetic stirring bar. The flask was then sealed with a rubber septum and it was evacuated and back filled with argon, twice. Degassed monomer was then added through a cannula. The ligand was then added and the solution was stirred until the copper complex formed. After the complex formation, the pyrene based initiator was added and the mixture was stirred at room temperature. After the predetermined time interval, the polymerization was stopped by dilution with THF. The polymer was precipitated using hexane/methanol and was dried under vacuum. The copper complex in the polymer was removed by passing the polymer solution in THF through a neutral alumina column. The solution obtained was used for the determination of molecular weight and PDI.

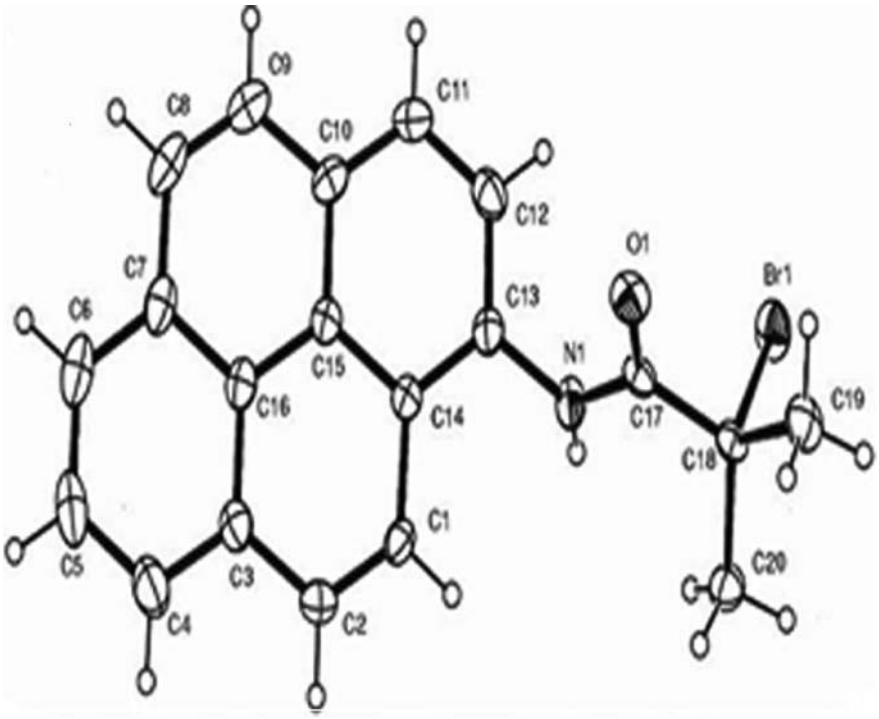

Fig. 1. Single Crystal X-ray Diffraction ORTEP image of Pyrene-derived initiator.

2.6 Synthesis of Block Copolymers via ATRP

The required quantity of the copper catalyst and the PS or PMMA macroinitiator was added to a flame dried Schlenk tube equipped with a magnetic stirring bar. The flask was then sealed with a rubber septum and it was evacuated and back filled with argon, twice. The mixture of solvent acetone and anisole (6:4 by volume) or tetrahydrofuran and the degassed monomer of interest was then added through a cannula. The ligand PMDETA or HMTETA was then added and the solution was stirred until the copper complex formed. Polymerization was performed at room temperature or at 90°C (wherever applicable) for the desired period of time. The product was purified by passing through Al_2O_3 column and then precipitated into hexane or methanol/water mixture. The resulting polymers were characterized by ^{1}H-NMR, GPC, IR, SEM and TGA measurements.

2.7 Synthesis of CdS Stabilized Amphiphilic Block Copolymer

P(S-*b*-AA) (0.033g) amphiphilic block copolymer was dissolved in 5 ml of DMF under vigorous stirring for 0.5 h. Cadmium acetate dihydrate (0.0456 g) in 0.5 ml of a mixture of methanol and DMF (1:2 v/v) was added to the polymer solution, under stirring at room temperature. A light blue solution was formed to which 20 ml of sodium sulphide ($Na_2S.9H_2O$) aqueous solution was added slowly. The solution was stirred vigorously under nitrogen atmosphere, in the dark over night, at room temperature. An aqueous golden yellow coloured solution of P(S-*b*-AA) -capped CdS nanoparticles was obtained.

3 Results and Discussions

In an attempt to investigate some of the physical properties of amphiphilic block copolymers, metal catalyzed atom transfer radical polymerization (ATRP) of monomers such as MMA and styrene were carried out, in solution condition, at ambient and higher temperatures (27). For this purpose, a novel ATRP initiator (R-X) with a pyrene endgroup was synthesized as shown in Scheme 1. It was characterized by ^{1}H, ^{13}C-NMR, Mass, DEPT spectroscopies and single crystal X-ray diffraction (SXRD) studies. The structure of pyrene derived initiator was determined by single crystal X-ray determination. The ORTEP diagram is shown in Figure 1. The interesting feature of the crystal structure is that there is a weak Br-Br intermolecular interaction [3.537(3) Å], which is shorter than the sum of the van der Waals radius of the Br atoms. The crystal structure is further stabilised by N-H...O and C-H...O interactions,where the oxygen atom (O1) forms a bonding with both N1-H1A and C20-H20C in a form of bifurcated bonding as shown in Figure 2.

The macroinitiators based on poly(methyl methacrylate) [PMMA-X] and poly(styrene) [PS-X] of relatively narrow molecular weight distribution were synthesized by exploring the experimental variables, as detailed in the

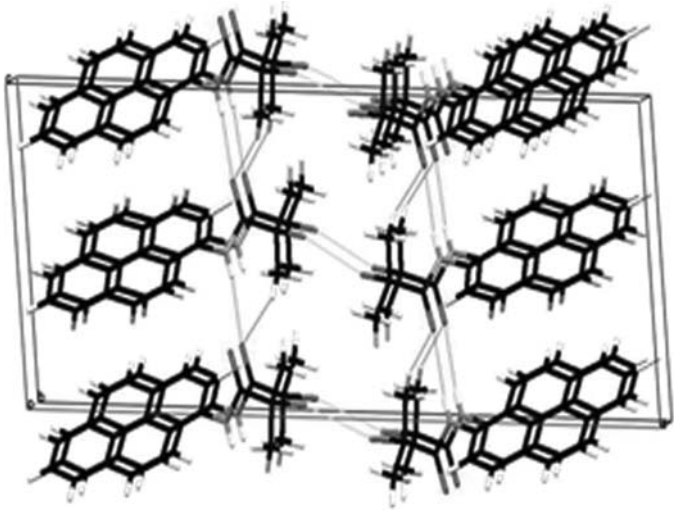

Fig. 2. Crystal Stabilization Structure of Pyrene based initiator; the crystal is stabilized by N-H...O, C-H...O and weak Br-Br interactions.

Tables 1–3. The block copolymers, P(S-*b*-*t*-BA)-Br, P(S-*b*-DMAEMA)-Br and P(MMA-*b*-DMAEMA) were successfully synthesized by ATRP yielding well defined diblock copolymers with polydispersities (M_w/M_n) < 1.5, as shown in Tables 1, 2 and 3. The diblock copolymers P(MMA-*b*-DMAEMA) were synthesized at ambient temperature from PMMA macroinitiator with CuBr/HMTETA catalyst. The details of the synthesis and molecular weight characteristics are given in Table 3. In general, the PDI is observed to increase upon polymerizing the second monomer. The PDI values are seen to increase from around 1.28 to 1.4–1.5 suggesting that the rate of block copolymerization is smaller than its initiation.

The TGA of the block copolymer P(S-*b*-DMAEMA) and P(MMA-*b*-DMAEMA) shows decomposition around 280°C, corresponding to the DMAEMA block and a broad transition occurring from 330 to 460°C, corresponding to the PS block. The TGA of the block copolymer P(MMA-*b*-DMAEMA) shows decomposition around 280°C, corresponding to DMAEMA block and a broad transition

Table 1. GPC characteristics of poly(styrene-*b*-*tert*-butyl acrylate) block copolymers

S. No	*First block*	*Block copolymer*	*M_n GPC*	*PDI*
1	PS^{a}_{115} M_n(GPC) = 12,000 PDI =1.28	PS_{115}-*b*-*t*-BA^{c}_{163}	32900	1.40
2	PS^{a}_{115} M_n (GPC) = 12,000 PDI =1.28	PS_{115}-*b*-*t*-BA^{b}_{281}	48000	1.43
3	PS^{a}_{115} M_n (GPC) = 12,000 PDI =1.28	PS_{115}-*b*-*t*-BA^{d}_{385}	61300	1.50

[a][Initiator]:[CuBr]:[HMTETA] =1:1:1 in DMF (25% v/v) at 90°C
[b][PS-Br] :[CuBr]:[PMDETA] = 1:1:1 in Anisole (50% v/v) at 90°C
[c][PS-Br]:[CuCl]:[PMDETA] =1:1:1 in Anisole (50% v/v) at 90°C
[d][PS-Br]:[CuCl]:[PMDETA] =1:1:1 in Anisole (50% v/v) at 90°C

Table 2. GPC characteristics of poly(S-*b*−DMAEMA) block copolymers

S. No	*First block*	*Block copolymer*	*M_n GPC*	*PDI*
1	PS^{a}_{336} M_n GPC = 35000 PDI = 1.29	PS_{336}-*b*-$DMAEMA^{c}_{113}$	52800	1.5
2	PS_{336} M_n GPC = 35000 PDI = 1.29	PS_{336}-*b*-$DMAEMA^{d}_{114}$	53000	1.40
3	PS^{b}_{115} M_n GPC = 12,000 PDI = 1.28	PS_{115}-*b*-$DMAEMA^{e}_{353}$	67600	1.48
4	PS_{115} M_n GPC = 12,000 PDI = 1.28	PS_{115}-*b*-$DMAEMA^{f}_{146}$	35000	1.45

a) [Initiator]:[CuBr]:[HMTETA] = 1:1:1 in DMF (25% v/v) at 90°C
b) [Initiator]:[CuBr]:[HMTETA] = 1:1:1 in DMF (25% v/v) at 90°C
c) [PMMA-Br]:[CuBr]:[HMTETA] = 1:1:1 in THF (25% v/v) at 90°C
d) [PMMA-Br]:[CuCl]:[HMTETA] = 1:1:1 in DMF (25% v/v) at 90°C
e) [PMMA-Br]:[CuBr]:[HMTETA] = 1:1:1 in DMF (25% v/v) at 90°C
f) [PMMA-Br]:[CuCl]:[HMTETA] = 1:1:1 in DMF (25% v/v) at 90°C

Table 3. GPC characteristics of poly(MMA-*b*−DMAEMA) block copolymers

S. No	*First block*	*Block copolymer*	*M_n GPC*	*PDI*
1	$PMMA^{a}_{120}$ M_n GPC = 12,000 PDI =1.23	$PMMA_{120}$-*b*-$DMAEMA^{c}_{14}$	14200	1.18
2	$PMMA^{b}_{56}$ M_nGPC = 5600 PDI = 1.29	$PMMA_{56}$-*b*-$DMAEMA^{d}_{26}$	9700	1.20
3	$PMMA_{56}$ M_nGPC = 5600 PDI =1.29	$PMMA_{56}$-*b*-$DMAEMA^{e}_{16}$	8200	1.40
4	$PMMA_{56}$ M_n GPC = 5600 PDI = 1.29	$PMMA_{56}$-*b*-$DMAEMA^{g}_{23}$	9300	1.31
5	$PMMA_{56}$ M_n GPC = 5600 PDI =1.29	$PMMA_{56}$-*b*-$DMAEMA^{f}_{51}$	13700	1.30

a) [Initiator]:[CuCl]:[PMDETA] =1:1:1 in DMF (50% v/v) at RT
b) [Initiator]:[CuCl]:[PMDETA] =1:1:1 in DMF (50% v/v) at RT
c) [PMMA-Br]:[CuBr]:[HMTETA] =1:1:1 in bulk at RT
d) [PMMA-Br]:[CuBr]:[HMTETA] =1:1:1 in bulk at RT
e) [PMMA-Br]:[CuCl]:[HMTETA] =1:1:1 in bulk at RT
f) [PMMA-Br]:[CuBr]:[HMTETA] =1:1:1 in THF 50% v/v at 90°C
g) [PMMA-Br]:[CuCl]:[HMTETA] =1:1:1 in Anisole 50% v/v at 90°C

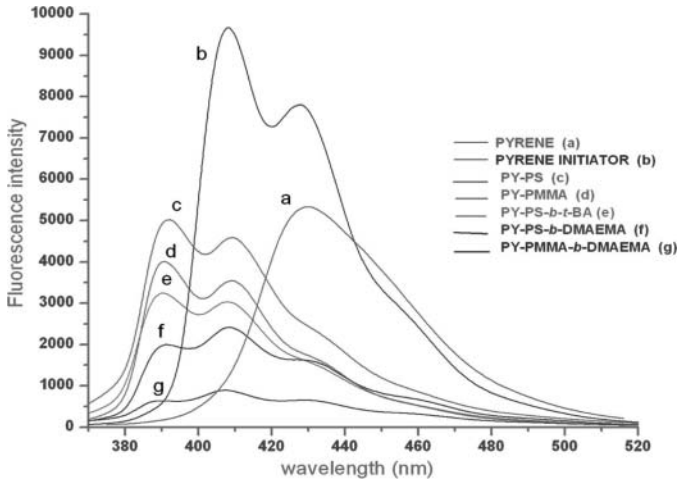

Fig. 3. Fluorescence emission spectra of block copolymers in DMF; 10^{-5} mol/L (excited at 337 nm).

occuring from 330 to 460°C, corresponding to the PMMA and PS blocks.

The polymers with a block of poly (*tert*-butyl acrylate) was hydrolyzed to poly(acrylic acid) by using trifluoroacetic acid as the catalyst in DCM at room temperature (28).

3.1 Fluorescence Studies

The fluorescence emission spectra of the small molecules used (1-aminopyrene and pyrene based ATRP initiator) and polymers were recorded in DMF, at the concentration of 10^{-5} mols/litre, as shown in Figure 3. The emission spectrum of 1-aminopyrene is very broad and consists of overlapping bands. The fluorescence spectrum of pyrene originates from the L_b state and has a long lifetime (> 450 ns), where L_a and L_b are the lower most electronic states of pyrene. A direct transition to L_b state is symmetry forbidden (therefore this shows very low absorption) and therefore the transitions to L_a state dominates the absorption spectrum. The amino group at the 1-position, as well as the subsequent introduction of the ATRP initiator brings about a significant perturbation in the molecular symmetry of 1-aminopyrene and hence absorption, as well as emissions show overlapping bands with fluorescence proceeding mostly through allowed transitions (life time measurement is in progress). In addition, the broadening could also be due to emission from the excimer. The emission spectrum of the ATRP initiator is less broad and shows two distinguishable peaks at 410 and 435 nm. The emission at 435 nm can be attributed to the excimer, while that 410 nm can be attributed to the pure initiator.

All the emissions from the polymers (Figs. 3c to 3g) are blue shifted. These spectra show three emission bands centered around 390 nm, 410 nm and 435 nm, which may be attributed to the emission from the monomeric pyrene units. The pyrene units in the polymer are surrounded by the macromolecular coil and hence the relaxations from the first excited electronic state to higher vibrational levels of the ground electronic state are seen clearly. All the polymers show similar intensity except Py-P(MMA_{56}-*b*-$DMAEMA_{26}$), which may be attributed due to the poor interaction of the polymer in DMF.

3.2 Swelling Studies

The swelling property of the amphiphilic block copolymers, P(S-*b*-DMAEMA), were investigated at different pH^s. The swelling ratio (SR) of the hydrogel was measured after it was immersed in the solvent of choice for the desired period of time. It was carefully taken out from the solution, wiped with a filter paper for the removal of the free water on the surface, and then weighed. The swelling ratio (SR; g/g) of a sample was calculated as follows: $SR = (w_t - w_d)/w_d$, where w_d and w_t are the weights of dry and wet samples at time t, respectively. When a hydrogel reaches its swelling equilibrium state under a fixed condition, its SR is called equilibrium swelling ratio (ESR). All measurements were made in triplicate, for each sample. The equilibrium swelling ratio, Q, is defined as the weight of the swollen gel divided by the weight of the same gel, before swelling. Swelling is expected due to the polymer segment – water interaction between the block copolymer with the buffer solutions, at different pH^s, at ambient temperature.

The water uptake ratio as a function of time was carried out for the block copolymers (different block length) synthesized, at three different pHs. In all the cases, the water uptake ratio increases linearly with time initially and thereafter saturation was observed. For the P(S-*b*-DMAEMA) block copolymer sample (Table 2), the swelling behavior is also seen to be dependent on the structure of the sample, which abruptly changes with pH. It is hypothesized that the gel formation is due to the uptake of water inside the structure resulting in the formation of a pseudo crosslinked structure. The swelling behaviour is found to be dependent on the composition of the hydrophilic moiety of the polymer, with Q increasing with increasing composition. At a pH of 4, the hydrogel is more hydrophilic due to the protonation of the amino group that results in a more extended conformation and hence the water uptake is high. At pH 4, most of the amino group exists as positive charged (N^+ $(CH_3)_2$) species. The positively charged amino groups, along the backbone exert repulsive force, which consequently expands the conformation and hence can take up more water. The equilibrium swelling ratio is also dependent on the content of the amino group and increases with the content of the hydrophilic moiety, as shown in Figure 4. At a pH of 7, the equilibrium swelling ratio is comparable with that at pH of 4, when the relative composition of the hydrophobic polystyrene part is on the higher side (Fig. 4). At a pH of 9.2, the hydrogel is not ionized and exhibits a relatively low degree of swelling due to the suppression of the dissociation of the amino moiety in the

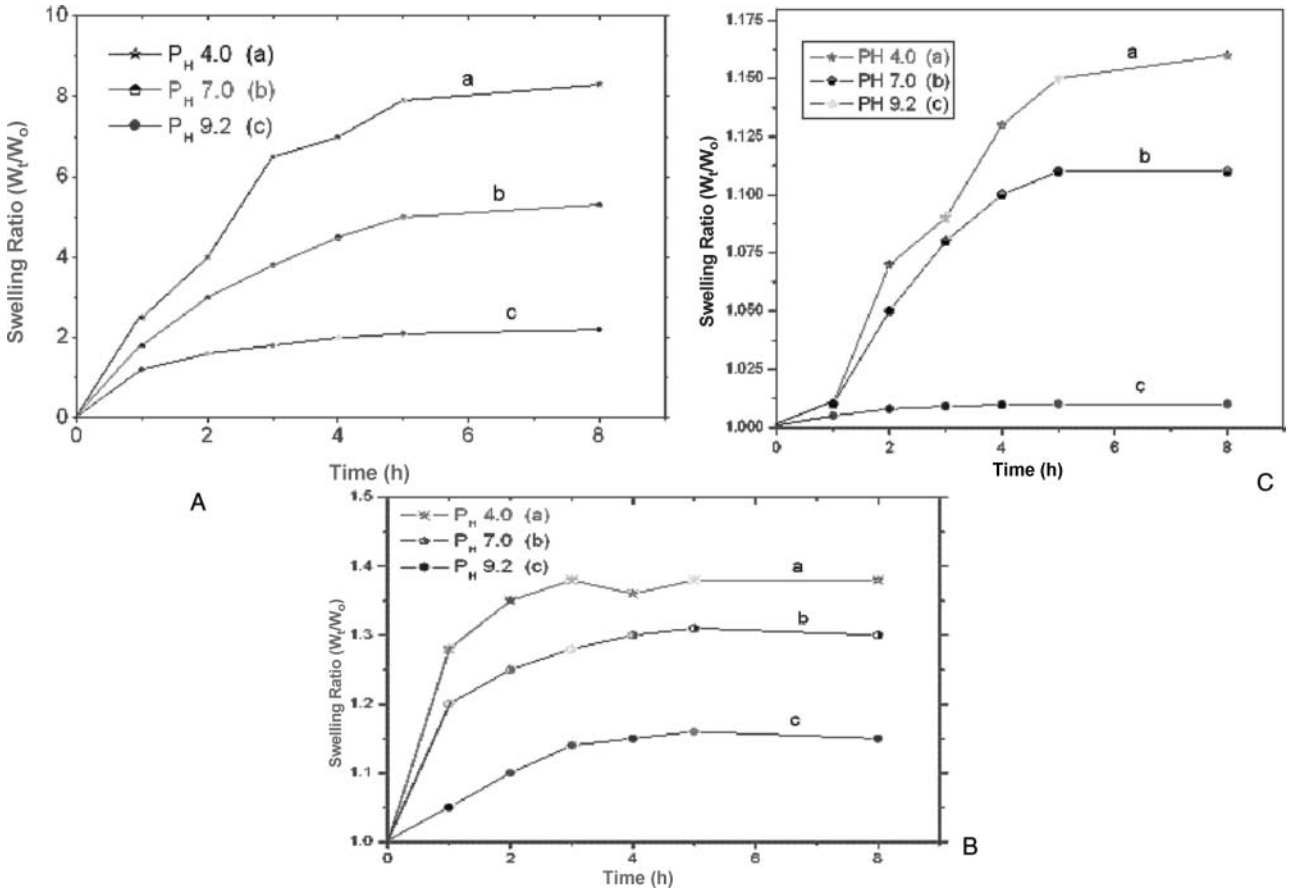

Fig. 4. Swelling ratio of the amphiphilic block copolymers at different pHs (● - pH = 9.2,♦ - pH = 7.0 and * - pH = 4.0). (PS_{115}-*b*-$DMAEMA_{353}$) (A); (PS_{115}-*b*-$DMAEMA_{146}$) (B); (PS_{336}-*b*-$DMAEMA_{114}$) (C).

DMAEMA block and the pseudo cross linked structure collapses. As a result, most of the P(DMAEMA) chains are rigid. Therefore the swelling ratio is lower than that in the neutral solution.

3.3 Morphological Studies

The morphological studies of the block copolymers and amphiphilic block copolymer capped CdS were studied using SEM measurements. The SEM image of the block copolymer P(S-*b*-*t*-BA) spin coated from DMF shows the self assembly of block copolymers, which produces hollow spheres like structure, that may be attributed to the *tert*-butyl block and the SEM images of block copolymers P(S-*b*-DMAEMA) spin coated from DMF, produces fine mosaic tiles like micro array which may be attributed to the formation of spherical domains of diameter 1.5 μm-0.3 μm, from the DMAEMA block, which are not shown here. The SEM images of block copolymers P(MMA-*b*-DMAEMA) spin coated from DMF, produces fine leaf like microarray, which could be attributed to the DMAEMA block with the formation of rope–like domains as shown in Figure 5(a). The SEM images of block copolymers P(S-*b*-AA) spin coated from DMF, produces a fine needle like microarray, which may be attributed to the acrylic acid block in which there is a conversion of spherical domains to fine needles after the hydrolysis (Fig. 5(b)).

The pyrene labeled fluorescent amphiphilic block copolymer can be used for the stabilization of CdS nanoparticle and for monitoring its presence through fluorescence. Block copolymer stabilized CdS nanoparticle was synthesized as described in the experimental section. The structures of the amphiphilic block copolymer capped CdS was confirmed by means of UV-Vis. and IR spectroscopies and morphological studies. The UV-Vis. absorption spectroscopy is one of the most frequently used methods to determine the size of CdS nanoparticles. The absorption band develops at approximately 500 nm, indicating the formation of large nanocrystals with a diameter of several nanometers. The molecular structure of the amphiphilic block copolymer capped CdS was also characterized by fourier- transform infrared spectroscopy. The observation of an intense peak at 3400 (N-H stretch) confirms the expected structure. The weak absorption observed at 405 cm^{-1} is due to the Cd-S bond, which are not shown here.

The powder x-ray diffraction pattern of amphiphilic block copolymer capped CdS is shown in Figure 6. The diffraction pattern exhibits prominent peaks at 2θ values

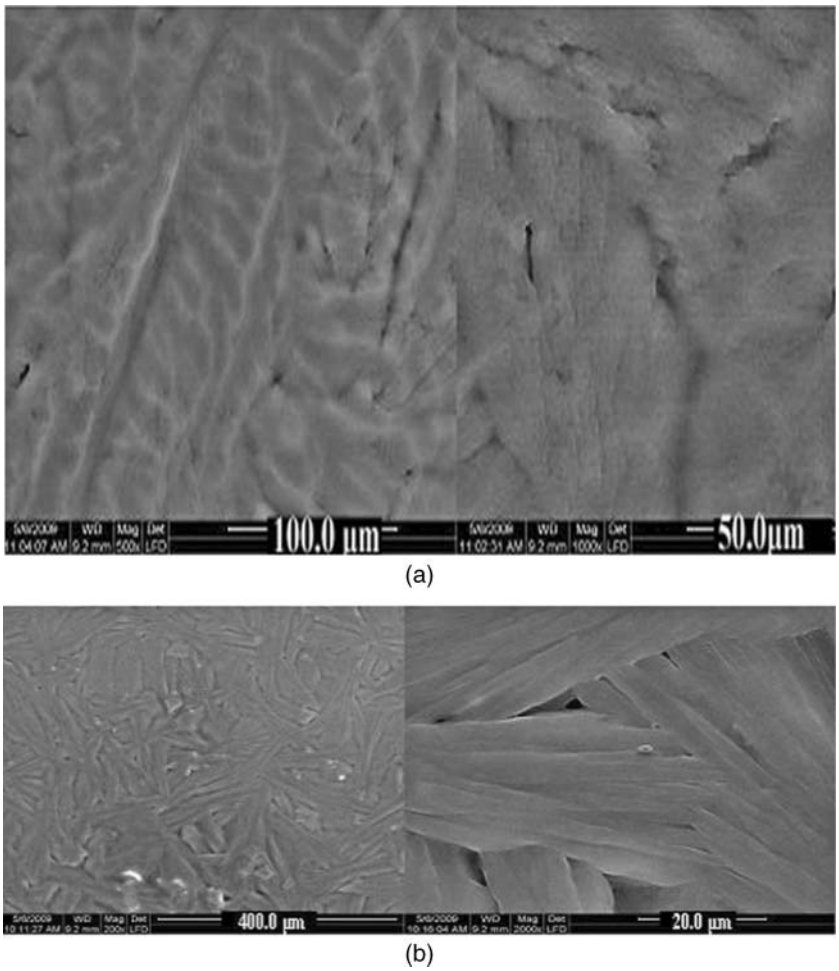

Fig. 5. SEM images of the block copolymer P(MMA_{56}-*b*-$DMAEMA_{26}$), in DMF solution coated with OsO_4 concentration of 10 mg/mL, at different magnifications (spin coated on to microscopic glass slide). (b) SEM images of the block copolymer P(S-*b*-AA), in DMF solution coated with OsO_4 concentration of 10 mg/mL, at different magnifications (spin coated on to microscopic glass slide).

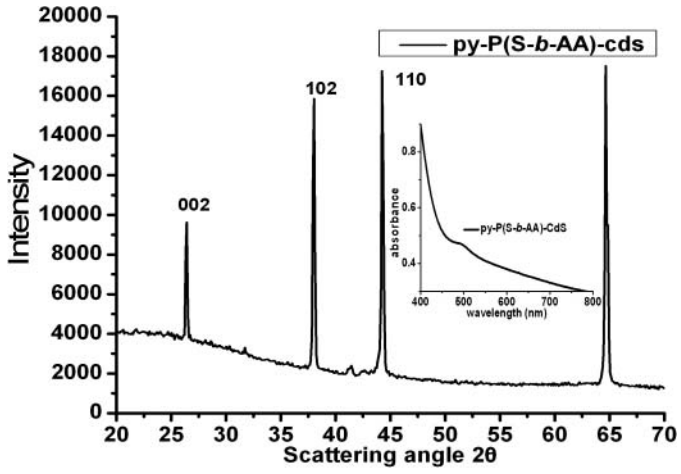

Fig. 6. Powder X-ray pattern of amphiphilic block copolymer [P(S-*b*-AA)] capped CdS. Inset: The UV-Vis. absorption spectroscopy of amphiphilic block copolymer [P(S-*b*-AA)] capped CdS in aqueous solution.

of 26.5 (002), 38.2 (102), 44.1 (110) and 65.0 due to Bragg reflections of CdS confirming that crystalline nanoparticles are presently stabilized by the polymer. The peak width at half maximum indicates that the material is in the nanometric size regime with a predominantly hexagonal phase. The compound showed blue shift in their UV-Visible absorption spectrum with the band edge at approximately 500 nm. Particle size was determined from the width of XRD peaks using Debye-Scherrer's formula

$$D = \frac{K\lambda}{\beta \cos \theta}$$

where β is the full width half maximum (FWHM), θ is the diffraction angle, d is the average crystalline size, λ is the wavelength of X-rays and K is the crystallite- shape factor and is equal to 0.9. The X-ray wavelength or λ for CuK_α is equal to 1.5418 Å. The estimated X-ray grain size of the polymer-nanoparticle as obtained from the Debye Scherrer formula from the FWHM of the peak corresponding to

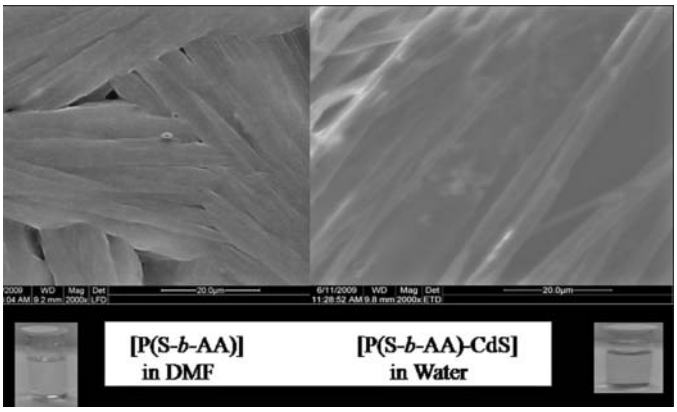

Fig. 7. SEM images of the amphiphilic block copolymer [P(S-*b*-AA)] capped CdS, in aqueous solution; at different magnifications (spin coated on to microscopic glass slide).

$2\theta = 26.5$ gives a rough estimation of the particle diameter to be 20.3 nm.

The SEM images of amphiphilic block copolymer capped CdS P(S-*b*-AA) - CdS spin coated from water, produces fine "coconut tree leaves like" structure, which may be attributed to the capping of CdS (Fig. 7.). The chemical composition of the amphiphilic block copolymer capped CdS was determined by X-ray energy dispersion analysis (EDAX). The typical EDAX spectrum for the synthesized polymeric nanoparticle reveals that the polymer–nanoparticle composite consisting of C, O, Cd and S. Quantitative analysis result indicates that the particle are indeed composed of Cd^{2+} and S^{2-} and at the same time, the atomic composition is more or less 1:2 of Cd and S, which may be attributed to the presence of unreacted sulphur in the composite.

4 Conclusions

A novel pyrene based ATRP initiator with the intrinsic tendency to function as a fluorescence marker is synthesized and characterized. The structure of the initiator is established by single crystal X-ray diffraction. The synthesis of novel, fluorescent, amphiphilic block copolymers with well defined molecular weight and reasonably narrow polydispersity $M_w/M_n < 1.5$ is achieved by ATRP, at ambient and higher temperatures. The characterization of the block copolymer, the fluorescence property and morphology were investigated. All the block copolymers exhibits fluorescence with distinct emissions at 390 nm, 410 nm and 435 nm for excitation at 337 nm and therefore would be useful as fluorescence markers. The SEM studies reveal unique morphologies for P(MMA-*b*-DMAEMA) and P(S-*b*-AA), which could be due to the end capping of pyrene moiety. The amphiphilic block copolymers based on DMAEMA monomer are observed to form pseudo gel*s* in aqueous solution with higher swelling capacity under acidic pH conditions. The stabilization of CdS nanoparticle was achieved by the interaction of the amphiphilic block copolymer as confirmed by UV-Vis. and IR spectroscopies and morphology studies.

References

1. Wang, J. and Matyjaszewski, K. (1995) *J. Am. Chem. Soc.*, 117(20), 5614–5615.
2. Solomon, D.H., Rizzardo, E. and Cacioli, P. (1985) *US Patent*, 4581429.
3. Kato, M., Kamigaito, M., Sawamoto, M. and Higashimura, T. (1995) *Macromolecules*, 28(5), 1721–1723.
4. Wang, J.S. and Matyjaszerwski, K. (1995) *Macromolecules*, 28(23), 7901–7910.
5. Tsolakis, K., Kallitsis, K. and Tsitsilianis, C. (2002) *J. Macromol. Sci., Part A: Pure Appl. Chem.,* 39(3), 155–169.
6. Chong, Y.K., Le, T.P.T., Moad, G., Rizzardo, E. and Thang, S.H. (1999) *Macromolecules*, 32(6), 2071–2074.
7. Ramakrishnan, A. and Dhamodharan, R. (2003) *Macromolecules*, 36(4), 1039–1046.
8. Harihara Subramanian, S. and Dhamodharan, R. (2008) *Polym. Int*., 57(3), 479–487.
9. Siu-Choon, N.G., Hang-Fang, L.U. and Chan, S.O. (2001) *Macromolecules*, 34(20), 6895–6903.
10. Leonard-Latour, M., Morelis, R.M. and Coulet, P.R. (1996) *Langmuir*, 12(20), 4797–4802.
11. Duhamel, J., Kanagalingam, S., O'Brien, T.J. and Ingratta, M.W. (2003) *J. Am. Chem. Soc.*, 125(42), 12810–12822.
12. Behanna, H.A., Rajangam, K. and Stupp, S.I. (2007) *J. Am. Chem. Soc.,* 129(2), 321–327.
13. Zhang, Y., Yang, W., Wang, C. and Fu, S. (2004) *Colloid Polym. Sci.,* 282(12), 1323–1328.
14. Winnik, F.M., Adronov, A. and Kitano, H. (1995) *Can. J. Chem*., 73(11), 2030–2040.
15. Nakayama, M. and Okano, T. (2005) *Biomacromolecules*, 6(4), 2320–2327.
16. Scales, C.W., Convertine, A.J. and Cormick, M.C. (2006) *Biomacromolecules*, 7(5), 1389–1392.
17. Laukkanen, A., Valtola, L., Winnik, F. M. and Tenhu, H. (2005) *Polymer*, 46(18), 7055–7065.
18. Erdogan, M., Hepuzur, Y., Cianga, I., Yagci, Y. and Pekcan, O. (2003) *J. Phys. Chem. A.,* 107(40), 8363–8370.
19. Chen, W.H., Liaw, D.J., Wang, K.L., Lee, K.R. and Lai, J.Y. (2009) *Polymer*, 50(22), 5211–5219.
20. Matyjaszewski, K. and Mueller, L. (2008) *Macromolecules,* 41(4), 1067–1069.
21. Adams, J. and Young, I. (2008) *J. Polym. Sci., Part A: Polym. Chem*., 46(18), 6082–6090.
22. Xue, L., Agarwal, U.S. and Lemstra, P.J. (2002) *Macromolecules*, 35(22), 8650–8652.
23. Adams, M.L., Lavasanifer, A. and Kwon, G.S. (2003) *J. Pharm. Sci.,* 92(7), 1343–1355.
24. Rosler, A., Vandermeulen, W.M. and Anton Klok, H. (2001) *Adv. Drug Delivery Rev.*, 53(1), 95–108.
25. Eychmuller, A. (2000) *J. Phys. Chem. B*., 104(28), 6514–6528.
26. Chen, K., Yang, Y., Sa, Q., Shi, L. and Zhao, H. (2008) *Polymer*, 49(11), 2650–2655 .
27. Vivek, A.V. and Dhamodharan, R. (2007) *J. Polym. Sci., Part A: Polym. Chem*., 45(17), 3818–3832.
28. Cheng, G., Boker, A. and Muller, H.E. (2001) *Macromolecule,* 34(20), 6883–6888.